CHEMISTRY OF MATERIALS

ARTICLE

pubs.acs.org/cm

Phloroglucinol Based Microporous Polymeric Organic Frameworks with −OH Functional Groups and High CO_2 Capture Capacity

Alexandros P. Katsoulidis and Mercouri G. Kanatzidis*

Department of Chemistry, Northwestern University, 2145 Sheridan Road, Evanston, Illinois 60208-3113, United States

Supporting Information

ABSTRACT: A new family of microporous polymeric organic frameworks (POF)s is described. The POFs are assembled from phlorglucinol (1,3,5-trihydroxybenzene) and several benzaldehyde derivatives under solvothermal conditions using Bakelite type chemistry of forming C−C bonds without any catalyst. The materials exhibit semiconductor-like optical absorption properties with energy gaps in the range of 1.5−2.5 eV. The new materials form as uniform, microporous, spherical particles and exhibit surface areas up to 917 $m^2 g^{-1}$. The micropores have a very uniform size as the gas adsorption isotherms of these amorphous materials are similar to those of crystalline microporous zeolites. The micropores are internally decorated with a large number of −OH reactive groups which are available for functionalization. The POFs capture as much as 18% of their mass of CO_2 at atmospheric pressure which is significantly larger than other porous polymers including systems which exhibit much larger surface areas; sodium-functionalized POFs exhibit enhanced heat of adsorption for H_2 of 9 kJ/mol compared to pristine POF at 8.3 kJ/mol.

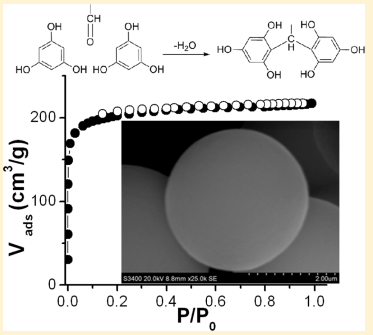

KEYWORDS: porous materials, microporous polymer, H_2 absorption, gas separation, gas storage

INTRODUCTION

The development of metal organic frameworks (MOFs) has opened a new synthetic pathway for ordered and tunable microporous frameworks based on coordination chemistry.[1,2] These materials are promising for applications in several fields such as gas storage, catalysis, and separations.[3−5] Considerable interest is also focused on structures composed entirely of light elements, such as covalent organic frameworks (COFs) and microporous organic polymers.[6,7] The former are high surface area crystalline frameworks prepared via polymerization of boronic acids, while the latter are disordered networks of various rings whose inefficient packing lead to open porous structures. The most developed family of microporous polymers is the hypercross-linked polymers (HPCs) developed by Davankov et al. and later expanded upon by many groups.[8] The microporosity in HPCs is created by the insertion of small molecules between the chains of a swollen or dissolved polymer such as polystyrene, polyarylate, or polyaniline, which are then cross-linked with Friedel−Crafts alkylation. In a different approach, so-called polymers of intrinsic microporosity (PIMs) have been constructed by connecting nonplanar rigid subunits having a spirocenter or a triptycene monomer.[9] Conjugated microporous polymers (CMPs) are a large family of compounds that combine high surface areas with physical properties relevant to extended conjugation. They are mainly synthesized by Sonogashira-Hagihara cross-coupling chemistry.[10] Also, several microporous polymers have been prepared by coupling[11,12] and other condensation reactions.[13−20] Among them, PAF-1 is distinguished for its very high BET surface area (5600 $m^2 g^{-1}$);[11] the triazine based CTF-1 and the imine linked COF-300 are known as crystallines of microporous organic polymers.[13,14] In the detailed review by McKeown and Budd all known synthetic methodologies about microporous organic polymers and their properties are presented.[20]

Here we describe a different approach to inducing microporosity involving phenolic resin-inspired chemistry. Phenolic resins comprise a large family of polymers which are produced by the reactions of phenolic molecules with formaldehyde or other aldehydes, with Bakelite being one of the earliest members of this family. Phenolic molecules have reactive sites suitable for electrophilic aromatic substitution, and they are linked through the formaldehyde carbon, followed by elimination of a molecule of H_2O. These reactions are catalyzed by acids or bases, and depending on the ratio of phenol to formaldehyde, the obtained resins are categorized into two groups—novolacs and resols.[21] Novolacs derive from an excess of phenol under neutral to acidic conditions, while basic reaction conditions using an excess of formaldehyde result in resols. Resols have been used widely as precursors for organic aerogels[22,23] and porous carbons.[24,25]

Here we report the synthesis of a new class of microporous polymeric organic frameworks (POFs) based on the reactions of phloroglucinol (1,3,5-trihydroxybenzene) with various benzaldehydes. The new phloroglucinol-based POFs are obtained in high yield without using any catalyst. These POFs have surface areas up to 917 $m^2 g^{-1}$ and exhibit high isosteric heat of H_2 adsorption at low coverage (9 kJ mol^{-1}). The materials are capable of capturing up to 18% and 9.5% by mass CO_2 at 273 and

Received: November 8, 2010
Revised: February 25, 2011
Published: March 16, 2011

298 K, respectively, at atmospheric pressure. The POFs possess large numbers of reactive −OH groups in their micropores which are available for further functionalization.

EXPERIMENTAL SECTION

Synthetic Protocol. All starting materials and solvents were purchased from Sigma-Aldrich Co. and used without further purification.

POF1A. In a Teflon lined autoclave were transferred 0.504 g (4 mmol) of phloroglucinol, 0.402 g (3 mmol) of terephthalaldehyde **1**, and 5 mL of dioxane. The autoclave was purged by N_2 to remove the air and placed in an oven at 220 °C for 4 days. After cooling at room temperature, a dark red solid was obtained and washed twice with THF. The solid was dried in vacuum oven at 50 °C. Yield: 86%.

POF2A. The same procedure as above was followed using 0.706 g (3 mmol) of 4-(4-formylphenoxy)benzaldehyde **2** instead of terephthalaldehyde. The color of the obtained solid was light brown. Yield: 81%.

POF3A. The same procedure as above was followed using 0.678 g (2 mmol) of tris(4-formylphenyl)amine **3** instead of terephthalaldehyde. The color of the solid was black. Yield: 63%.

POF1B. In a round-bottom flask an amount of 0.504 g (4 mmol) of phloroglucinol and 0.402 g (3 mmol) of terephthalaldehyde **1** were added in 5 mL of dioxane. The mixture was kept under stirring at 70 °C for 1 h. The obtained yellow solution was then transferred to a Teflon lined autoclave which was purged by N_2 to remove the air and placed in an oven at 220 °C for 4 d. After cooling at room temperature, a dark red solid was collected by filtration and washed twice with THF. The solid was dried in a vacuum oven at 50 °C. Yield: 94%.

POF2B. The same procedure as for POF1B was followed by using 0.706 g (3 mmol) of 4-(4-formylphenoxy)benzaldehyde **2** instead of terephthalaldehyde. The color of the solid was light brown. Yield: 87%.

POF3B. The same procedure as for POF1B was followed by using 0.252 g (2 mmol) of phloroglucinol and 0.339 g (1 mmol) of tris-(4-Formylphenyl)amine **3** in 5 mL of dioxane. In this case half concentrations of reactants compared to POF1B and POF2B were used in dioxane in order to get a clear solution. The color of the solid was black. Yield: 71%.

POF1B(MeONa). 0.2 g of dry POF1B was dispersed in ethanol. After 10 min, 0.2 mL of MeONa (25% in methanol) was added to the dispersion and allowed to react for 1 h. The dispersion was filtered and washed with ethanol.

POF Stability Tests in Water. Three parts of 100 mg of POF1B were soaked in 100 mL of deionized water, in HCl aqueous solution of pH = 1, and in NaOH aqueous solution of pH = 13, respectively. Those mixtures were stirred at room temperature for 24 h. The polymers were then collected by filtration and dried in a vacuum oven at 50 °C. The new samples are called POF1B(1), POF1B(7), and POF1B(13), where the number in parentheses reflects the pH of the solution. Part of POF1B-(13) was retreated in HCl aqueous solution of pH = 1 and is denoted as POF1B(13−1).

Physical Characterization. N_2 adsorption−desorption isotherms were measured at 77 K. The specific surface area was calculated according to the BET method ($0.01 < P/P_0 < 0.1$). The micropore volume was determined by Dubinin−Radushkevich. Non-local density functional theory (NLDFT), the cylindrical model, was applied to obtain the pore size distribution.[26] CO_2 adsorption isotherms were measured at 273 K, and the specific surface area was estimated by Dubinin−Radushkevich. H_2 adsorption isotherms were measured at 77 and 87 K. For all adsorption measurements, a Micromeritics ASAP 2020 porosimeter was used. Before each measurement, the sample was degassed for 10 h at 120 °C under high vacuum.

Solid state magic angle spinning NMR spectra were recorded in a Varian 400 ATX spectrometer operating 100 MHz for ^{13}C and 400 MHz for ^{1}H. The ^{13}C CPMAS measurements were carried out at a spinning rate of 10 kHz. Two pulse phase modulation (TPPM) ^{1}H decoupling was applied during acquisition. The ^{13}C chemical shifts are given relative to tetramethylsilane as zero ppm and calibrated by using adamantine as a secondary reference. The obtained spectra were interpreted with the software iNMR 3.3 Mesterlab Research (http://www.inmr.net).

Scheme 1. (a) Starting Materials, (b) Polymerization Reaction between Carbonyl Group and Phloroglucinol (1,3,5-trihydroxybenzene), and (c) Fully Condensed Structure between Dialdehyde 1 and Phloroglucinol

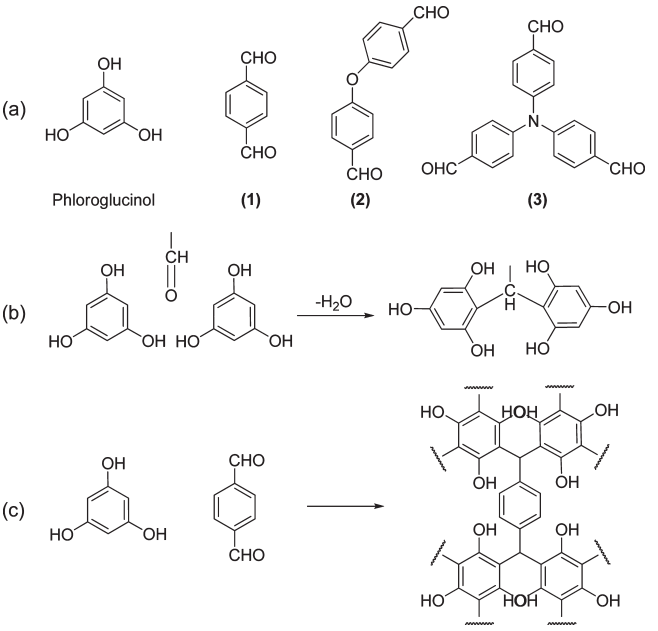

FT-IR spectra were measured by diffuse reflectance (DRIFT) method after mixing a part of each sample with KBr. The measurements were carried out in a Thermo Nicolet 6700 spectrometer under nitrogen atmosphere by averaging 128 scans from 4000 to 400 cm^{-1} with a resolution of 2 cm^{-1}.

UV−vis−NIR diffuse reflectance spectra (DRS) were recorded with a Shimadzu UV-3101PC spectrophotometer. $BaSO_4$ powder was used as the 100% reflectance standard. The reflectance data were converted to absorption according to the Kubelka−Munk equation $a/S = (1 - R)^2/2R$, where R is the reflectance and a and S are the absorption and scattering coefficient, respectively.[27]

Thermogravimetric analysis was performed in a Shimadzu TGA-50 thermal analyzer by heating each sample (∼10 mg) from room temperature to 600 °C with ramping rate of 5 °C min^{-1} under nitrogen flow.

Scanning electron microscopy (SEM) images were collected in a Hitachi S-3400N instrument with an accelerating voltage of 20 kV. High magnification SEM images were collected on a Leo 1525 (Carl Zeiss Microimaging Inc.). Before measurement, the samples were sputter coated with gold.

RESULTS AND DISCUSSION

We synthesized POFs by the reaction of phloroglucinol with the dialdehydes **1** and **2** and trialdehyde **3** (Scheme 1a). The phloroglucinol molecule is highly reactive for electrophilic aromatic substitution because of the electron donating resonance effect of the three hydroxyl groups. The carbonyl group is

Table 1. Porous Properties of Phloroglucinol-Based POFs and Yield of Synthesis

sample	specific surface area ($m^2\ g^{-1}$)	micropore volume ($cm^3\ g^{-1}$)	mean pore diameter (Å)	Yield (%)
POF1A	773	0.27	6	86
POF1B	917	0.36	6	94
POF2A	658	0.23	6	81
POF2B	769	0.27	6	87
POF3A	115 (415)[a]	0.04 (0.17)[a]		63
POF3B	608 (582)[a]	0.22 (0.22)[a]	6	71
POF1B(MeONa)	589	0.22	6	

[a] Amounts estimated by CO_2 adsorption.

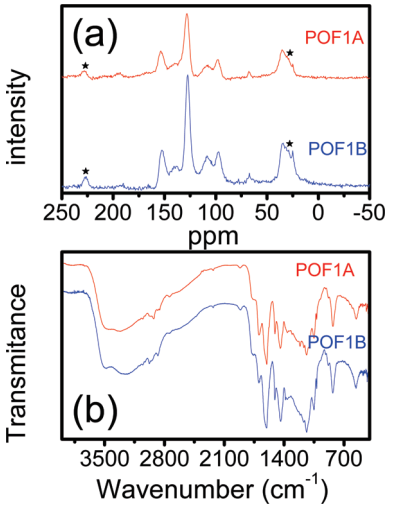

Figure 1. (a) Solid state ^{13}C CPMAS-NMR spectra of POF1A and POF1B. Asterisks denote the spinning sidebands. (b) FTIR spectra of POF1A and POF1B.

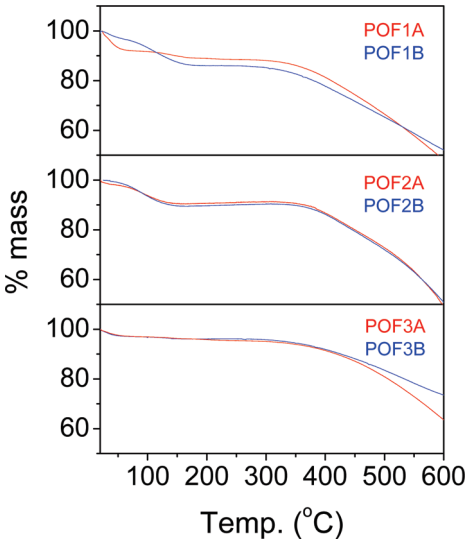

Figure 2. TGA curves for all POF samples under N_2 flow.

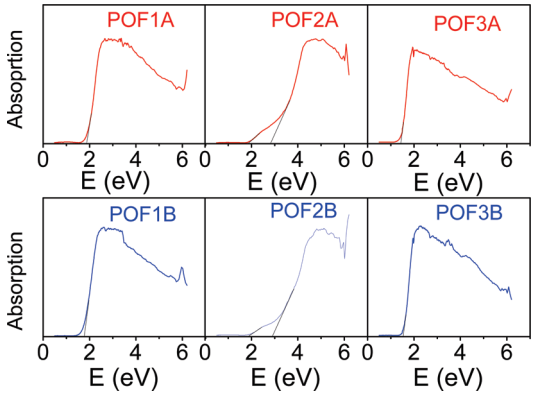

Figure 3. Solid state absorption spectra for all POF samples.

attacked by the electron-rich phenyl rings and links with two phloroglucinol molecules by eliminating a water molecule (Scheme 1b). Dialdehydes **1** and **2** can react with four phloroglucinol molecules and trialdehyde **3** with six of them. At the same time, each phloroglucinol molecule can react with three aldehyde molecules (Scheme 1c). All polymerization reactions were carried out under solvothermal conditions at 220 °C for four days and followed one of two synthetic routes. In synthetic protocol A, the reactants and dioxane were mixed directly in the autoclave. In protocol B, reactants and dioxane were mixed and left to react in a flask for 1 h at 70 °C before transferring in the autoclave for further reaction at higher temperature. This preliminary step facilitates the mixing of monomers and enhances yield of each reaction (Table 1).

The polymeric frameworks were characterized with solid state magic angle spinning NMR spectroscopy. The ^{13}C CP-MAS NMR spectra of POF1A and POF1B show the resonance peaks related to the covalent linking of phloroglucinol and dialdehyde **1** (Figure 1a). The resonance at 35 ppm is assigned to the tertiary carbon formed by the condensation reaction, and the peak at 108 ppm corresponds to reacted phloroglucinol ortho-carbons. On the other hand, the signal at 98 ppm is attributed to unreacted phloroglucinol ortho-carbons, indicating that the condensation is not fully completed. The peak at 128 ppm originates from the aromatic carbons, while the peak at 153 ppm comes from the phenoxy carbons. The methyne bridge carbon is established by the presence of the resonance peak at 35 ppm, and the signal of phloroglucinol condensed ortho-carbons is shown as a shoulder overlapped by the peak of aromatic carbons at 120 ppm for POF2A and POF2B samples (Supporting Information Figure S1a). The weak peaks at 25 and 67 ppm indicate residues of THF trapped inside the micropores.

FTIR spectroscopy indicates the presence of terminal OH groups in these polymers. The stretching vibration mode of the O−H bond at ∼3500 cm^{-1} as well as the characteristic for hydrogen bonding broad absorbance between 3400 and 2900 cm^{-1} is present in all spectra (Figure 1b and Supporting Information Figure S2a−b). Finally, the low intensity peak at 1700 cm^{-1} is assigned to residual unreacted aldehyde groups.

The POFs are stable on heating under N_2 until 350 °C, and they retain more than 50% of their mass at 600 °C as revealed by thermogravimetric analysis (Figure 2). All samples show mass loss around 10% up to 150 °C attributed to solvent evaporation (dioxane, H_2O, and THF), all of which are trapped in micropores and were not removed by the drying procedure. POF1A and POF1B are dark red and exhibit strong light absorption in the

dx.doi.org/10.1021/cm103206x |*Chem. Mater.* 2011, 23, 1818–1824

visible region that corresponds to band gaps of ~1.8 eV. The POF2A and POF2B are light brown and present two band gaps at 1.9 and 2.8 eV. POF3A and POF3B are black with an optical band gap of 1.5 eV. The solid state absorption spectra are given in Figure 3. POF1A and POF1B as well as POF3A and POF3B show strong semiconductor-like light absorption which probably is the result of extensive electron delocalization within the polymeric framework.

N_2 adsorption−desorption isotherms of POF1A and POF1B are given in Figure 4a. They correspond to type I isotherms according to IUPAC classification[28] and reveal the microporous character of these materials. However, the type I isotherms of these POFs resemble those of classic microporous crystalline materials such as small pore zeolites; the POFs however are completely amorphous as revealed by the X-ray diffraction experiments (Supporting Information Figure S3). The specific surface area is estimated at 773 and 917 $m^2 g^{-1}$ for POF1A and POF1B, respectively. From the robust porous features of the six materials, which are presented in Table 1, it is concluded that the smaller dialdehyde molecule **1** condenses with phloroglucinol to create open frameworks of higher microporosity. Also, the initial synthetic step in the flask (samples synthesized with method B) increases the surface area of the solids in all cases. A N_2 condensation step is observed for the samples POF2A and POF2B (Supporting Information Figure S5a) at relative pressures $P/P_0 > 0.95$, which is a clear indication of macroporosity in these samples. The POF3A exhibits unexpectedly low N_2 adsorption, and the BET specific surface area is calculated as 115 $m^2 g^{-1}$ (Supporting Information Figure S5b). Interestingly, when the POF3A sample was investigated by CO_2 adsorption at 0 °C, it showed a better defined isotherm shape (Supporting Information Figure S5c) with a calculated surface area at 415 $m^2 g^{-1}$. This is attributed to a case of very narrow micropores that are accessible by CO_2 molecules but not by N_2 molecules. The kinetic diameter of CO_2 at 3.3 Å is smaller than that of of N_2 at 3.64 Å.[29] A similar phenomenon has been observed in several other kinds of microporous materials, such as activated carbons, MOFs, and polymers.[30] POF3B does not show a significant difference in specific surface area measurement between N_2 (608 $m^2 g^{-1}$) and CO_2 (582 $m^2 g^{-1}$). Hysteresis between adsorption and desorption branches is observed for some samples, and it

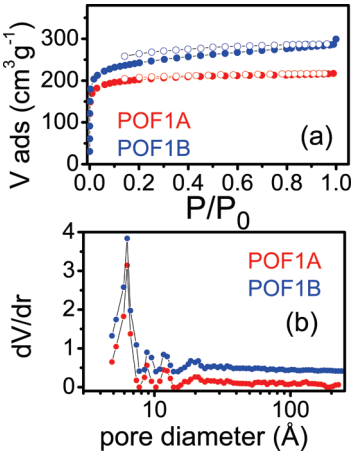

Figure 4. (a) N_2 adsorption desorption isotherms at 77 K for POF1A and POF1B (closed symbols correspond to adsorption points and open symbols to desorption points). (b) Pore size distribution analysis according to NLDFT for POF1A and POF1B.

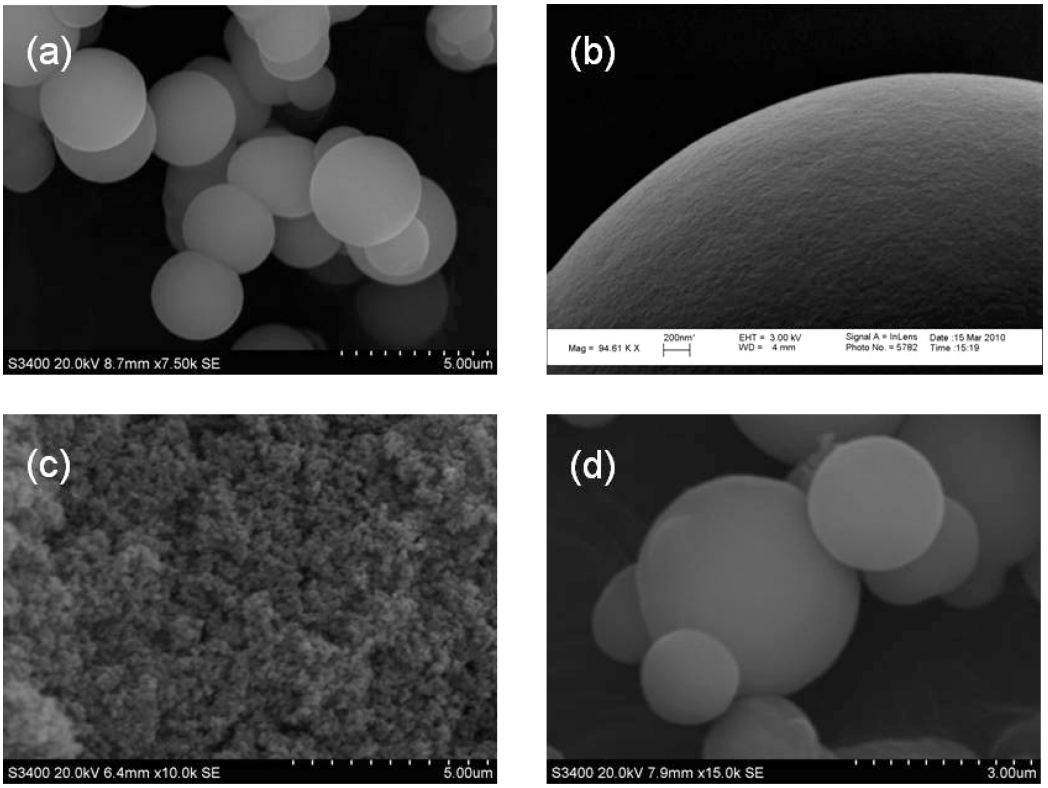

Figure 5. (a, c, d) SEM images of POF1B, POF2B, and POF3B respectively. (b) High magnification SEM image of POF1B.

dx.doi.org/10.1021/cm103206x |*Chem. Mater.* 2011, 23, 1818–1824

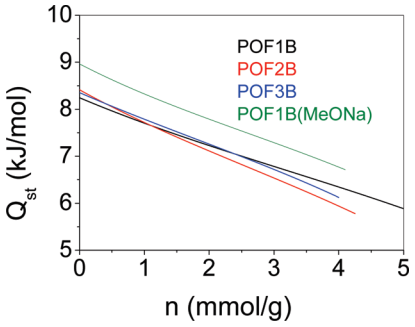

Figure 6. Isosteric heat of H_2 adsorption for POF1B, POF2B, POF3B, and POF1B(MeONa).

does not close at low pressures. However, the hysteresis at low relative pressure is hard to explain. For microporous organic materials hysteresis is attributed to elastic deformations of soft framework that occurred during adsorption.[9a,31] For all samples except POF3A, the pore size distribution results show a maximum at 6 Å and several smaller peaks between 9 and 13 Å, proving their definite microporous character (Figure 4b and Supporting Information Figure S6).

The morphology of the POFs was examined with SEM. POF1A and POF1B, as well as POF3A and POF3B, consist of regular spherical particles with diameter 1−4 μm (Figure 5 and Supporting Information). The external surface of these spheres is very smooth as shown by the high magnification SEM image of POF1B (Figure 5b) and accounts for the absence of any N_2 condensation close to atmospheric pressure in the adsorption measurements as there are no macropores or cavities. Generally, we consider that these spheres consist of a continuous microporous framework. On the other hand SEM images of POF2A and POF2B (Figure 5c and Supporting Information) show random aggregates of tiny particles with diameter ~ 100 nm, creating interparticle porosity as it is suggested by the adsorption isotherms. The POF samples were also checked with TEM (Supporting Information p 19), but the small diameter of the pores and the amorphous character of the framework did not allow for the direct observation of any additional details.

The samples prepared with method B were investigated for H_2 and CO_2 storage properties. H_2 adsorption isotherms were obtained at low pressure at 77 K and 87 K. The uptake of H_2 varies from 1.25 wt % for POF1B to around 1 wt % for POF2B and POF3B (Supporting Information Figures S7a−c). The isosteric heat of H_2 adsorption was calculated as 8.3(2) kJ/mol at low coverage, falling to 5.8(2) kJ/mol for POF1B and POF2B and 6.1(2) kJ/mol for POF3B approaching the atmospheric pressure (Figure 6). The modified by sodium methoxide sample POF1B(MeONa) presented a higher heat of adsorption (9 kJ/mol) at low coverage. This could be attributed to a better enthalpic interaction of H_2 with Na^+ ions in the structure, similar to that suggested for the interaction of Li^+ ions.[32] However, a reduction of microporosity is observed after treatment with MeONa (Table 1) because of the presence of Na cations in the micropores of POFs.

CO_2 adsorption isotherms were collected at 273 K and 298 K, at pressures up to 1 bar (Figure 7). The results are plotted as adsorbed volume per mass, which is directly measured, as well as adsorbed mass per mass (calculated after measurement by ASAP 2020 v3.00 software) to compare them easily with other published results. What is noteworthy is all samples show significant

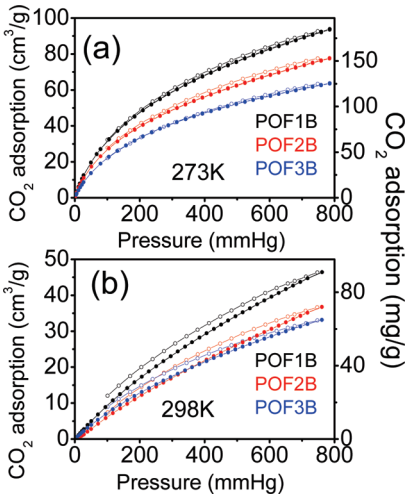

Figure 7. CO_2 adsorption−desorption isotherms at (a) 273 K and (b) 298 K of POF1B, POF2B, and POF3B. The adsorbed amount is presented as $cm^3\ g^{-1}$ on the left axis and as mg g^{-1} on the right axis.

Scheme 2. Substitution Reaction on POF1B by NaOH[a]

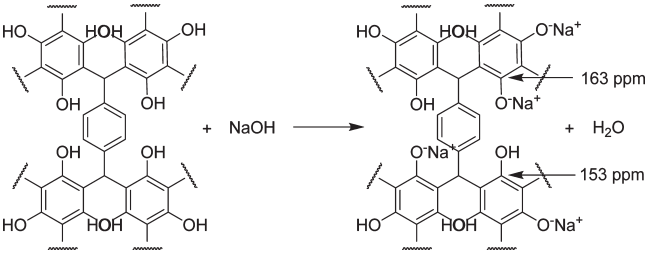

[a] The chemical shifts of different phenoxy carbons are given.

uptakes even though their surface areas are moderate and the adsorption process is reversible in all cases as the desorption branches are very close to that of adsorption. Remarkably, at 273 K, POF1B captures 94 $cm^3\ g^{-1}$, or 18 wt %, of CO_2 near atmospheric pressure (Figure 7a), which is a larger capacity than has been reported for COFs.[33] The highest CO_2 uptake of COFs is 85 $cm^3\ g^{-1}$ for COF-6; other COFs show lower CO_2 adsorption under the same conditions. Microporous polymers (ACMPs) prepared by Choi et al. exhibit CO_2 adsorption as much as 7 wt % at 273 K and 1 bar.[10e] At 298 K, POF1B adsorbs 48 $cm^3\ g^{-1}$ or 9.5 wt % CO_2 (Figure 7b), which is in the middle of the range of MOFs with high CO_2 capacity.[34] Meanwhile, recently published results for microporous polymers show a maximum CO_2 uptake of 7.6 wt % at 298 K and 1 bar.[35] Because of their purely microporous structure, the POFs described here exhibit outstanding CO_2 adsorption properties that are comparable with high surface area (>3000 $m^2\ g^{-1}$) materials such as MOFs, COFs, and microporous polymers.

The POF1B was checked for stability in water under neutral, acidic (pH = 1), and basic (pH = 13) conditions by soaking for 24 h. The neutral and acid treated samples retained their porosity at 90% and 85%, respectively, of the original surface area (Supporting Information Figure S10 and Table S1), and their optical properties were unaffected (band gap ~ 1.75 eV, Supporting Information Figure S9). When samples of POF1B were immersed in concentrated NaOH, we observed partial substitution of protons from the acidic OH groups by Na^+ cations

(Scheme 2). This is indicated by the presence of an extra peak in ^{13}C CP MAS NMR spectra at 163 ppm of phenoxy carbons as well as the original 153 ppm peak (Supporting Information Figure S12). The Na^+ cation polarizes the C−O bond, and as consequence this carbon is shifted downfield from 153 to 163 ppm by deshielding. The NaOH treated sample showed no porosity, and its energy band gap is decreased to 1.6 eV. The Na^+ cations could be removed by redispersion in acidic solution (pH = 1), indicating reversible ion-exchange properties. This is proved by EDS analysis, which indicated the absence of Na after HCl treatment, as well as by NMR and UV−vis spectroscopy (Supporting Information Figures S11 and S12). Namely, the resonance peak at 163 ppm disappeared, and the band gap returned to its original value of 1.73 eV.

■ CONCLUDING REMARKS

We have demonstrated a new class of microporous polymeric organic frameworks with OH functional groups which can be prepared by a straightforward route involving the reaction of phloroglucinol with aldehydes. The C−C linkages that create the networks are formed without any catalyst and provide remarkable stability in a broad range of pH values. Their particles exhibit spherical morphology and large numbers of functional hydroxyl groups that are available for ion exchange. These POFs are excellent CO_2 adsorbents, capturing up to 9.5% of their mass at ambient conditions, in comparison with 7.6% of other microporous polymers. The heat of H_2 adsorption and the interaction of the POFs with adsorbed H_2 is improved by functionalization with Na^+. The strong visible light absorption of the materials indicates a significant degree of π bond conjugation in their backbone which could render them attractive for investigation of their electronic properties. These materials are promising for scale up because of the rapid synthesis, low cost of the starting materials, and the absence of catalyst. We are exploring structure−property relationships for these types of materials, with the aim of further understanding their pore properties and exploring a variety of ion-exchange and gas adsorption applications.

■ ASSOCIATED CONTENT

Supporting Information. Solid state NMR and FTIR spectra, gas adsorption isotherms, heat of adsorption calculations, and TEM and SEM images (PDF). This material is available free of charge via the Internet at http://pubs.acs.org.

■ AUTHOR INFORMATION

Corresponding Author
*E-mail: m-kanatzidis@northwestern.edu.

■ ACKNOWLEDGMENT

Support by DOE-EERE is gratefully acknowledged (Grant No. DE-FG36-08GO18137/A001). We also thank Prof. R.Q. Snurr for helpful discussions.

■ REFERENCES

(1) Yaghi, O. M.; Li, H.; Davis, C.; Richardson, D.; Groy, T. L. *Acc. Chem. Res.* **1998**, *31*, 474.
(2) Eddaoudi, M.; Moler, D. B.; Li, H.; Chen, B.; Reineke, T. M.; O'Keeffe, M.; Yaghi, O. M. *Acc. Chem. Res.* **2001**, *34*, 319.
(3) Eddaoudi, M.; Kim, J.; Rosi, N.; Vodak, D.; Wachter, J.; O'Keeffe, M.; Yaghi, O. M. *Science* **2002**, *295*, 469.
(4) Czaja, A.; Turkhan, N.; Muller, U. *Chem. Soc. Rev.* **2009**, *38*, 1284.
(5) Lee, J. Y.; Farha, O. K.; Roberts, J.; Scheidt, K. A.; Nguyen, S. T.; Hupp, J. T. *Chem. Soc. Rev.* **2009**, *38*, 1450.
(6) Yaghi, O. M.; O'Keeffe, M.; Ockwig, N.; Chae, H. K.; Eddaoudi, M. *Nature* **2003**, *423*, 705.
(7) Maly, K. E. *J. Mater. Chem.* **2009**, *19*, 1781.
(8) (a) Davankov, V. A.; Tsyurupa, M. P. *React. Polym.* **1990**, *13*, 27. (b) Davankov, V. A.; Pastukhov, A. V.; Tsyurupa, M. P. *J. Polym. Sci., Part B: Polym. Phys.* **2000**, *38*, 1553. (c) Tsyurupa, M. P.; Davankov, V. A. *React. Funct. Polym.* **2002**, *53*, 193. (d) Wood, C. D.; Tan, B.; Trewin, A.; Niu, H. J.; Bradshaw, D.; Rosseinsky, M. J.; Khimyak, Y. Z.; Campbell, N. L.; Kirk, R.; Stockel, E.; Cooper, A. I. *Chem. Mater.* **2007**, *19*, 2034. (e) Germain, J.; Svec, F.; Frechet, J. M. J. *Chem. Mater.* **2008**, *20*, 7069. (f) Schwab, M. G.; Senkovska, I.; Rose, M.; Klein, N.; Koch, M.; Pahnke, J.; Jonschker, G.; Schmitz, B.; Hirscher, M.; Kaskel, S. *Soft Matter* **2009**, *5*, 1055.
(9) (a) McKeown, N. B.; Budd, P. M.; Msayib, K. J.; Ghanem, B. S.; Kingston, H. J.; Tattershall, C. E.; Maksheed, S.; Reynolds, K. J.; Fritch, D. *Chem.—Eur. J.* **2005**, *11*, 2610. (b) Ghanem, B. S.; Hashem, M.; Harris, K. D. M.; Msayib, K. J.; Xu, M.; Budd, P. M.; Chaukura, M.; Book, D.; Tedds, S.; Walton, A.; McKeown, N. B. *Macromolecules* **2010**, *43*, 5287.
(10) (a) Cooper, A. I. *Adv. Mater.* **2009**, *21*, 1. (b) Jiang, J. X.; Su, F.; Trewin, A.; Wood, C. D.; Niu, H.; Jones, J. T. A.; Khimyak, Y. Z.; Cooper, A. I. *J. Am. Chem. Soc.* **2008**, *130*, 7710. (c) Schmidt, J.; Weber, J.; Epping, J. D.; Antonietti, M.; Thomas, A. *Adv. Mater.* **2008**, *20*, 1. (d) Stöckel, E.; Wu, X.; Trewin, A.; Wood, C. D.; Clowes, R.; Campbell, N. L.; Jones, J. T. A.; Khimyak, Y. Z.; Adams, D. J.; Cooper, A. I. *Chem. Commun.* **2009**, 212. (e) Choi, J. H.; Choi, K. M.; Jeon, H. J.; Choi, Y. J.; Lee, Y.; Kang, J. K. *Macromolecules* **2010**, *43*, 5508.
(11) Ben, T.; Ren, H.; Ma, S.; Cao, D.; Lan, J.; Jing, X.; Wang, W.; Xu, J.; Deng, F.; Simmons, J. M.; Qiu, S.; Zhu, G. *Angew. Chem., Int. Ed.* **2009**, *48*, 9457.
(12) Chaikittisilp, W.; Sugawara, A.; Shimojima, A.; Okubo, T. *Chem.—Eur. J.* **2010**, *16*, 6006.
(13) Kuhn, P.; Antonietti, M.; Thomas, A. *Angew. Chem., Int. Ed.* **2008**, *47*, 3450.
(14) Uribe-Romo, F. J.; Hunt, J. R.; Furukawa, H.; Klock, C.; O'Keefe, M.; Yaghi, O. M. *J. Am. Chem. Soc.* **2009**, *131*, 4570.
(15) Schwab, M. G.; Fassbender, B.; Spiess, H. W.; Thomas, A.; Feng, X.; Mullen, K. *J. Am. Chem. Soc.* **2009**, *131*, 7216.
(16) Farha, O. K.; Spokoyny, A. M.; Hauser, B. G.; Bae, Y. S.; Brown, S. E.; Snurr, R. Q.; Mirkin, C. A.; Hupp, J. T. *Chem. Mater.* **2009**, *21*, 3033.
(17) Zhang, B.; Wang, Z. *Chem. Commun.* **2009**, 5027.
(18) Ren, H.; Ben, T.; Wang, E.; Jing, X.; Xue, M.; Liu, B.; Cui, Y.; Qiu, S.; Zhu, G. *Chem. Commun.* **2010**, 2091.
(19) Pandey, P.; Katsoulidis, A. P.; Eryazici, I.; Wu, Y.; Kanatzidis, M. G.; Nguyen, S. T. *Chem. Mater.* **2010**, *22*, 4974.
(20) McKeown, N. B.; Budd, P. M. *Macromolecules* **2010**, *43*, 5163.
(21) Lin-Gibson, S.; Riffle, J. S. In *Synthetic methods in step-growth polymers*; Rogers, M. E., Long, T. E., Eds.; John Wiley & Sons: Hoboken, NJ, 2003.
(22) Pekala, R. W. *J. Mater. Sci.* **1989**, *24*, 3221.
(23) Barral, K. *J. Non-Cryst. Solids* **1998**, *225*, 46.
(24) Nishiyama, N.; Zheng, T.; Yamane, Y.; Egashira, Y.; Ueyama, K. *Carbon* **2005**, *43*, 269.
(25) Meng, Y.; Gu, D.; Zhang, F.; Shi, Y.; Yang, H.; Li, Z.; Yu, C.; Tu, B.; Zhao, D. *Angew. Chem., Int. Ed.* **2005**, *44*, 7053.
(26) Details about methods of analysis for N_2 adsorption isotherms are given inRouquerol, F.; Rouquerol, J.; Sing, K. *Adsorption by powders & porous solids*; Academic Press: Marseille, 1999.
(27) (a) Wendlandt, W. W.; Hecht, H. G. *Reflectance Spectroscopy*; Interscience Publishers: New York, 1966. (b) Kortum, G. *Reflectance Spectroscopy: Principles, Methods, Applications*; Springer: Berlin, 1969. (c) Tandon, S. P.; Gupta, J. P. *Phys. Status Solidi* **1970**, *38*, 363. (d) Chondroudis, K.; McCarthy, T. J.; Kanatzidis, M. G. *Inorg. Chem.* **1996**, *35*, 840. (e) Liao, J. H.; Varotsis, C.; Kanatzidis, M. G. *Inorg. Chem.* **1993**, *32*, 2453.

(28) Sing, K. S. W.; Everett, D. H.; Haul, R. A. W.; Moscou, L.; Pierotti, P. A.; Rouquerol, J.; Siemieniewska, T. *Pure Appl. Chem.* **1985**, *57*, 603.
(29) Beck, D. W. *Zeolite Molecular Sieves*; Wiley: New York, 1974.
(30) (a) Garrido, J.; Linares-Solano, A.; Martin-Martinez, J. M.; Molina-Sabio, M.; Rodrigues-Reinoso, F.; Terregrosa, R. *Langmuir* **1987**, *3*, 76. (b) Dybtsev, D. N.; Chun, H.; Yoon, S. H.; Kim, D.; Kim, K. *J. Am. Chem. Soc.* **2004**, *126*, 32. (c) Jeon, Y. M.; Armatas, G. S.; Heo, J.; Kanatzidis, M. G.; Mirkin, C. A. *Adv. Mater.* **2008**, *20*, 2105.
(31) Weber, J.; Antonietti, M.; Thomas, A. *Macromolecules* **2008**, *41*, 2880.
(32) (a) Mulfort, K. L.; Hupp, J. T. *J. Am. Chem. Soc.* **2007**, *129*, 9604. (b) Li, A.; Lu, R. F.; Wang, Y.; Wang, X.; Han, K. L.; Deng, W. Q. *Angew. Chem., Int. Ed.* **2010**, *49*, 3330.
(33) Furukawa, H.; Yaghi, O. M. *J. Am. Chem. Soc.* **2009**, *131*, 8875.
(34) (a) Millward, A. R.; Yaghi, O. M. *J. Am. Chem. Soc.* **2005**, *127*, 17998. (b) D'Allesandro, D. M.; Smit, B.; Long, J. R. *Angew. Chem., Int. Ed.* **2010**, *49*, 6058.
(35) Holst, J. R.; Stockel, E.; Adams, D. J.; Cooper, A. I. *Macromolecules* **2010**, *43*, 8531.